

## Adsorption of Dicamba and MCPA onto MIL-53(Al) Metal-organic Framework: Response Surface Methodology and Artificial Neural Network Model Studies

Hamza Ahmad Isiyaka<sup>a\*</sup>, Khairulazhar Jumbri<sup>a</sup>, Nonni Soraya Sambudi<sup>b</sup>, Zakariyya Uba Zango<sup>a</sup>, Nor Ain Fathihah Abdullah<sup>a</sup>, Bahruddin Saad<sup>a</sup> Adamu Mustapha<sup>c</sup>

<sup>a</sup>Department of Fundamental and Applied Sciences, Universiti Teknologi PETRONAS, 32610 Seri Iskandar, Perak, Malaysia, [hamza\\_18001996@utp.edu.my](mailto:hamza_18001996@utp.edu.my); [khairulazhar.jumbri@utp.edu.my](mailto:khairulazhar.jumbri@utp.edu.my)

<sup>b</sup>Chemical Engineering Department, Universiti Teknologi PETRONAS, 32610 Seri Iskandar, Perak, Malaysia.

<sup>c</sup>Department of Geography, Faculty of Earth and Environmental Science, Kano University of Science and Technology, Wudil, 3244 Kano State, Nigeria

### Content List

1. Table S1: Coded range of independent variables for the CCD-RSM factor levels.
2. Table S2: Experimental design data matrix for predicting adsorption capacity of dicamba and MCPA
3. Table S3: Analysis of variance (ANOVA) for dicamba and MCPA adsorption by RSM
4. Table S4: Kinetics parameters for the adsorption of dicamba and MCPA onto MIL-53(Al)
5. Table S5 Isotherm parameters for dicamba and MCPA adsorption onto MIL-53(Al)
6. Table S6: Thermodynamic parameters for the adsorption of dicamba and MCPA onto MIL-53(Al)
7. Fig. S1: RSM prediction scatter plots (a) dicamba (b) MCPA, and ANN prediction scatter plots (c) dicamba (d) MCPA.
8. Fig. S2: Pseudo-second-order kinetics for adsorption capacity of (a) dicamba and (b) MCPA.
9. Fig. S3: Intraparticle diffusion model kinetics (a) dicamba and (b) MCPA.
10. Fig. S4: Freundlich isotherms for the removal of (a) dicamba and (b)

Table S1: Coded range for independent variables for the CCD-RSM factor levels

Variables	Units	Range and levels				
		- $\alpha$	-1	0	+1	+ $\alpha$
Contact time	min	35	5	15	25	45
Initial concentration	mg/L	40	10	20	30	50
Adsorbent dosage	g/L	0.04	0.01	0.02	0.03	0.05
pH		8	2	4	6	10
Temperature	°C	40	25	30	35	45

Table S2: Experimental design data matrix for predicting adsorption capacity of dicamba and MCPA

Runs	Contact time (min)	Initial concentration (mg/L)	Adsorbent dosage (g/L)	pH	Temperature (°C)
1	15	20	0.02	4	30
2	5	10	0.03	2	35
3	15	20	0.04	4	30
4	15	20	0.02	8	30
5	25	40	0.02	4	30
6	25	10	0.01	2	35
7	15	20	0.02	4	45
8	5	30	0.01	2	35
9	5	30	0.01	6	25
10	5	30	0.03	2	25
11	5	10	0.03	6	35
12	25	10	0.01	6	35
13	25	30	0.03	6	35
14	25	30	0.01	2	35
15	5	10	0.01	2	25
16	5	30	0.01	6	35
17	35	20	0.02	4	30
18	5	30	0.03	6	35
19	5	30	0.03	6	25
20	25	10	0.03	2	25
21	25	30	0.01	6	35
22	15	20	0.02	10	30
23	25	10	0.03	6	25
24	25	10	0.03	6	35
25	45	20	0.02	4	30
26	25	20	0.01	4	40
27	5	10	0.01	6	25
28	5	10	0.03	6	25
29	25	30	0.03	2	35
30	5	30	0.01	2	25
31	25	30	0.03	2	25
32	5	10	0.01	2	35
33	5	30	0.03	2	35
34	25	30	0.01	6	25
35	5	10	0.03	2	25
36	25	10	0.01	6	25
37	15	20	0.05	4	30

38	15	20	0.02	4	30
39	25	50	0.01	4	40
40	5	10	0.01	6	35
41	15	10	0.01	2	25
42	25	30	0.03	6	25
43	25	30	0.01	2	25
44	25	20	0.01	4	35

Table S3: Analysis of variance (ANOVA) for dicamba and MCPA adsorption by RSM

Source	Dicamba			MCPA			P-value			
	Sum of square	df	mean square	F-value	P-value	Sum of square	df	mean square	F-value	< 0.0001
Model	419.1	17	24.6	73.4	< 0.0	439.5	17	25.8	70.8	0.0
A-Time	4.4	1	4.4	13.2	0.0	5.4	1	5.4	14.8	< 0.0
B-Concentration	324.1	1	324.1	965.8	< 0.0	337.3	1	337.3	924.3	0.0
C-Dosage	2.6	1	2.6	7.7	0.0	2.7	1	2.7	7.5	0.1
D-pH	0.6	1	0.6	1.8	0.1	0.7	1	0.7	2.1	0.0
E-Temperature	2.1	1	2.1	6.2	0.0	2.3	1	2.3	6.4	0.0
AB	2.1	1	2.1	6.3	0.0	2.1	1	2.1	5.8	0.0
AC	4.6	1	4.6	13.8	0.0	5.2	1	5.2	14.4	0.0
AD	5.4	1	5.4	16.9	0.0	5.7	1	5.7	15.7	0.0
BC	3.7	1	3.7	11.1	0.0	3.9	1	3.9	10.9	0.0
BD	2.3	1	2.3	7.0	0.0	2.7	1	2.7	7.4	0.0
BE	1.3	1	1.3	3.8	0.1	1.4	1	1.4	3.9	0.0
CD	5.3	1	5.3	16.1	0.0	6.1	1	6.1	16.6	0.0
CE	3.2	1	3.2	9.7	0.0	3.5	1	3.5	9.7	0.0
DE	2.9	1	2.9	8.7	0.0	2.8	1	2.8	7.7	0.0
BĀ <sup>2</sup>	5.7	1	5.7	17.1	0.0	7.5	1	7.5	20.5	0.0
CĀ <sup>2</sup>	3.8	1	3.8	11.4	0.0	5.1	1	5.1	14.0	0.0
EĀ <sup>2</sup>	2.5	1	2.5	7.5	0.0	2.4	1	2.4	6.7	
Residual	4.3	26	0.3			4.7	26	0.3		
Lack of Fit	4.3	1	0.5			4.7	1	0.5		
Pure Error	0.0	25	0.0			0.0	25	0.0		
Cor Total	423.5	43				444.2	43			
	<b>Dicamba</b>			<b>MCPA</b>						
R <sup>2</sup>	0.988			0.987						
R <sup>2</sup> adj	0.974			0.976						
Predicted R <sup>2</sup>	0.866			0.870						
Adeq Precision	24.519			24.761						

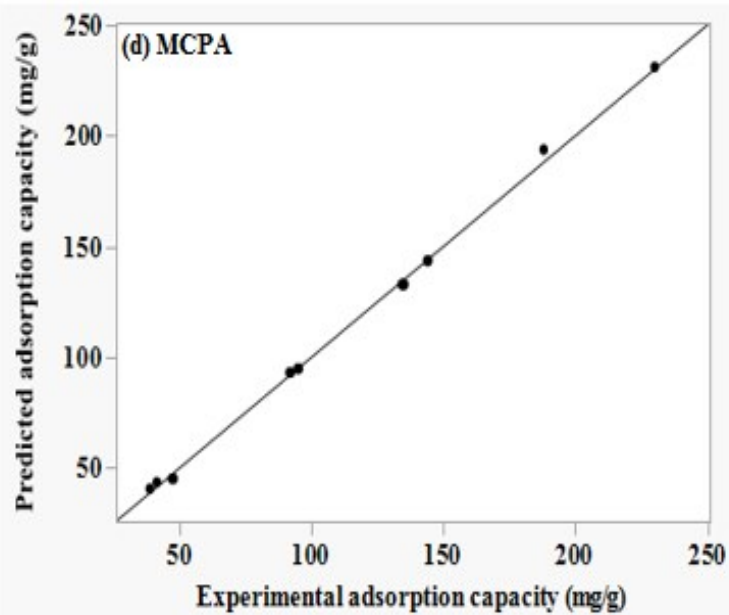
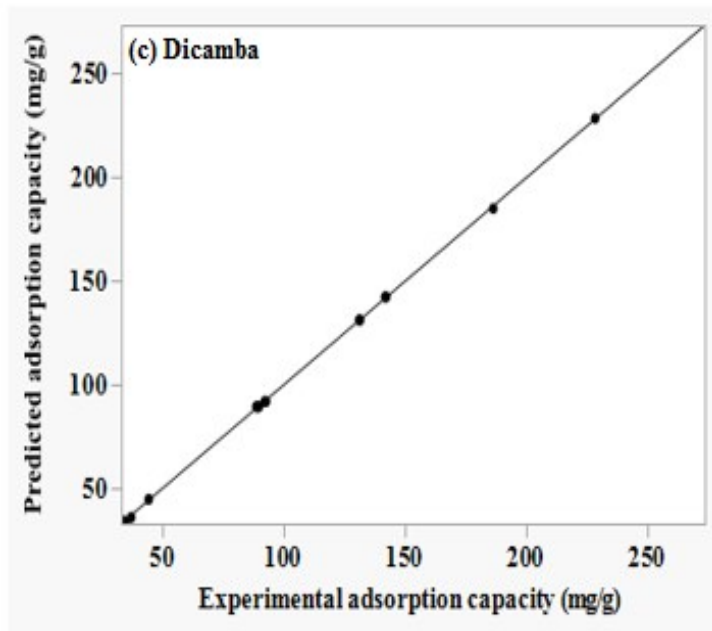
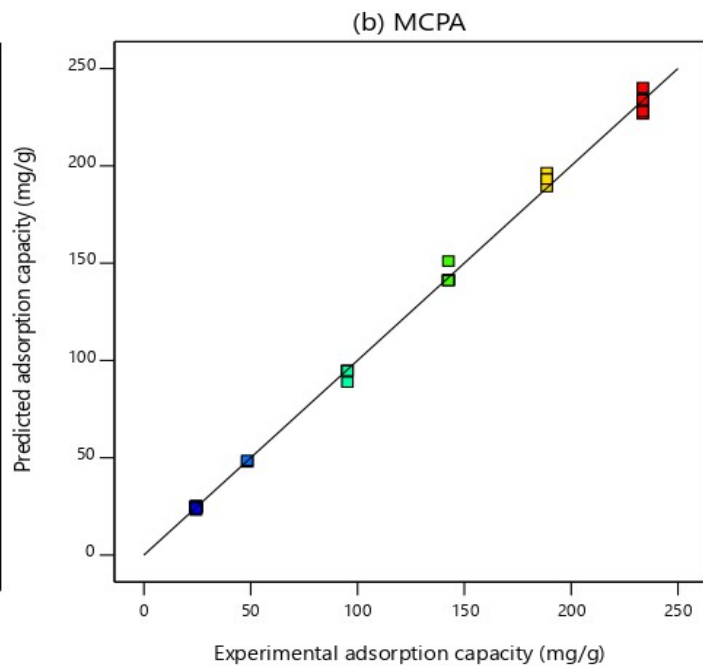
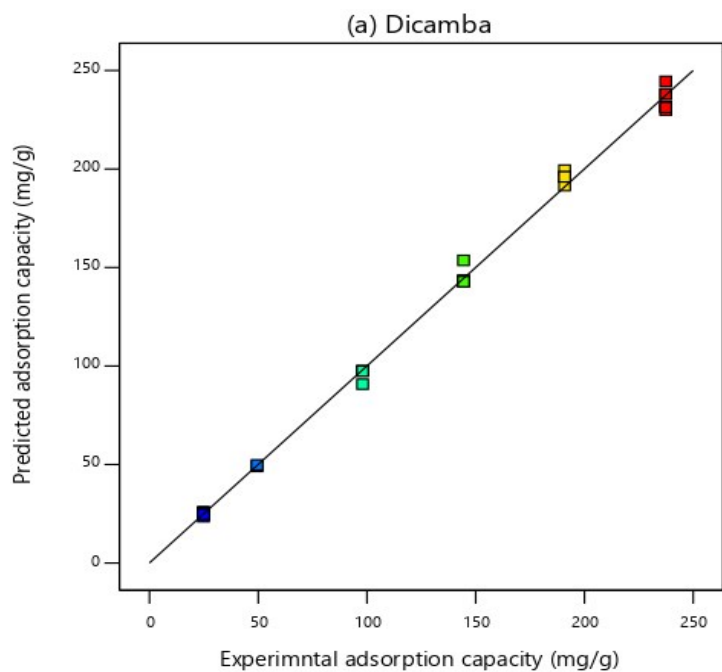


Fig. S1: RSM prediction scatter plots (a) dicamba (b) MCPA and ANN prediction scatter plots (c) dicamba (d) MCPA

### Adsorption Kinetics

Adsorption kinetics was applied to understand the rate of adsorbate uptake, reaction mechanism and equilibrium time required for the adsorption process. It is a fundamental factor that was used to determine the effectiveness and efficiency of the adsorbent as well as the mass transfer which explains the rate-limiting steps in designing the adsorption system<sup>1</sup>. In this study, the pseudo-first order, pseudo second order and intraparticle diffusion model were used to ascertain the best fitting for the experimental data. Using these models, criteria such as coefficient of determination (R<sup>2</sup>), adjusted R<sup>2</sup> (R<sup>2</sup>adj), root mean square error (RMSE), alkaikie information criteria (AIC) are considered as the best fit to judge the performance of our adsorption process by regression analysis<sup>2</sup>.

The following equations were used for this study<sup>1</sup>. The equations for the models were given as:

Lagergren pseudo-first-order model

$$q_t = q_e(1 - e^{-k_1 t}) \quad (11)$$

Pseudo-second-order model

$$q_t = \frac{K_2 q_e^2 t}{1 + K_2 q_e t} \quad (12)$$

Intraparticle diffusion model

$$q_t = K_p t^{0.5} + C \quad (13)$$

Where  $q_t$  and  $q_e$  are the amount of dicamba and MCPA adsorbed at certain equilibrium and time  $t$  (mg/g),  $K_1$  (min<sup>-1</sup>) is the pseudo-first-order rate constant,  $K_2$  (g mg/g min<sup>-1</sup>) is the equilibrium rate constant of the pseudo-second-order and the intraparticle diffusion rate constant is represented as  $K_p$  (mg/g min<sup>-1</sup>).

### Adsorption isotherms

Adsorption isotherms provide information on the adsorption capacity and the type of interaction mechanism that exist between MIL-53(Al) and the studied herbicides. The Langmuir, Freundlich and Temkin isotherms were used to describe the adsorption of dicamba and MCPA onto MIL-53(Al). The models are described by the following equations<sup>2</sup>:

Langmuir model

$$\frac{C_e}{q_e} = \frac{1}{K_L q_m} + \frac{C_e}{q_m} \quad (14)$$

$$R_L = \frac{1}{1 + C_e K_L} \quad (15)$$

Where  $C_e$  is the concentration at equilibrium (mg/g),  $q_e$  is the quantity of dicamba and MCPA adsorbed at equilibrium (mg/g),  $q_m$  and  $K_L$  are the constant representing adsorption capacity and adsorption energy, respectively.  $R_L$  depict the favourability of the adsorption process ( $R_L > 1$ , unfavourable;  $0 < R_L < 1$ , favourable;  $R_L = 1$ , linear).

Freundlich model

$$\log(q_e) = \log K_F + \frac{1}{n} \log C_e \quad (16)$$

Where  $K_F$  is the Freundlich constant of adsorption capacity,  $n$  is the adsorption intensity and  $C_e$  is the equilibrium concentration of dicamba and MCPA (mg/g).

Temkin model

$$q_e = B \ln A_T + B \ln C_e \quad (17)$$

Where  $B$  is the heat of adsorption (J/mol) and  $A_T$  is the Temkin equilibrium binding constant corresponding with the maximum binding energy (L/g).

### Thermodynamics studies

The basic thermodynamic parameters were used in this study to assess the feasibility of adsorption process based on temperature changes. They include the Gibbs free energy change ( $\Delta G^\circ$ ), enthalpy change ( $\Delta H^\circ$ ) and entropy change ( $\Delta S^\circ$ ). This helps to determine whether the adsorption process is spontaneous, exothermic or endothermic. The equations are given as <sup>3</sup>:

$$\Delta G^\circ = -RT \ln K_c \quad (18)$$

$$\Delta G^\circ = \Delta H^\circ - T \Delta S^\circ \quad (19)$$

Where  $\Delta G^\circ$  is the free energy (J K mol<sup>-1</sup>),  $T$  (K) and  $R$  (J K mol<sup>-1</sup>) are the temperature and universal gas constant for the adsorption, respectively and  $K_c$  is the equilibrium constant.

### Kinetics model

Kinetics parameters were studied using the pseudo-first-order, pseudo-second-order and intra-particle diffusion models to ascertain the best fitting model that describe the adsorption process. From all the values obtained for the various models, the pseudo-second-order kinetics (Fig. S2 (a) and (b)) has the best fitting between the experimental and the theoretical values with the coefficient of determination  $R^2 > 0.99\%$  for both dicamba and MCPA;  $R^2_{adj} > 0.99\%$ , lowest RMSE = 0.005, least AIC = - 133.830 values. The  $q_e$  values calculated for the pseudo-second-order kinetic model for dicamba and MCPA are in agreement with the experimental results in Table S4. The maximum  $q_e$  values for dicamba and MCPA were determined as  $q_{e \text{ exp.}}$  228.5, 231.9 mg/g and  $q_{e \text{ cal.}}$  227.2, 232.5 mg/g respectively at the equilibrium points which represent the adsorption capacity of MIL-53(Al). These values are in strong agreement with the RSM and ANN prediction models, which indicate that the simulated adsorption capacity by RSM and ANN is well validated by the experimental findings. Thus, the result further explain that the adsorption is a chemisorption process since it follows the pseudo-second-order kinetics. The intraparticle diffusion mechanism was used to describe the interaction and the movement of the molecules inside the particles of the adsorbent. Fig S3 (a) and b)) indicate two major stages that represent an external diffusion of herbicides to the surface of the adsorbent and the penetration of the molecules inside the pore of the MOF.

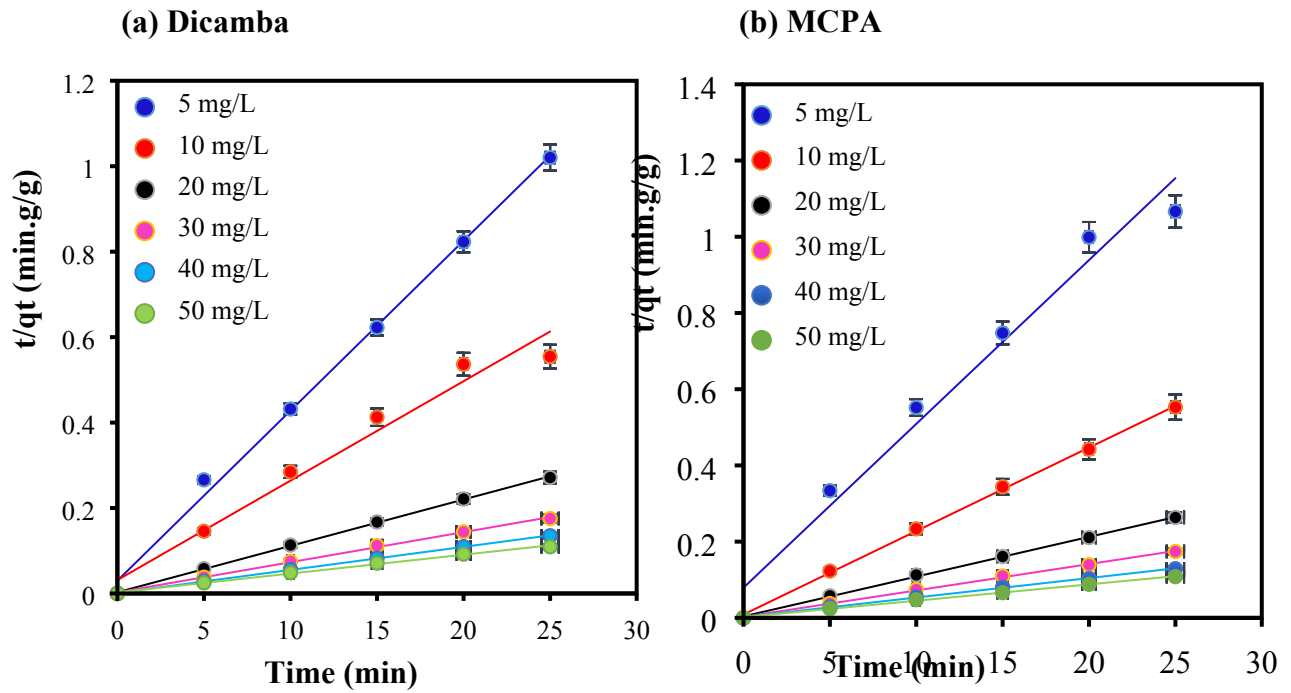
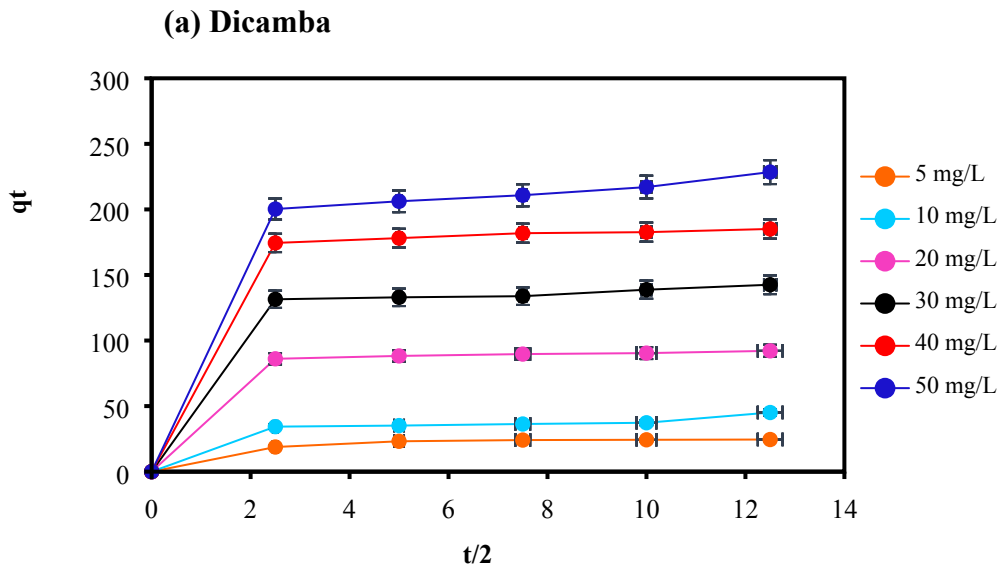


Fig. S2: Pseudo-second-order kinetics for the removal of (a) dicamba and (b) MCPA (Dosage: 0.01 g/L; 40°C; equilibrium time: 25 min; rpm: 150).



**(b)MCPA**

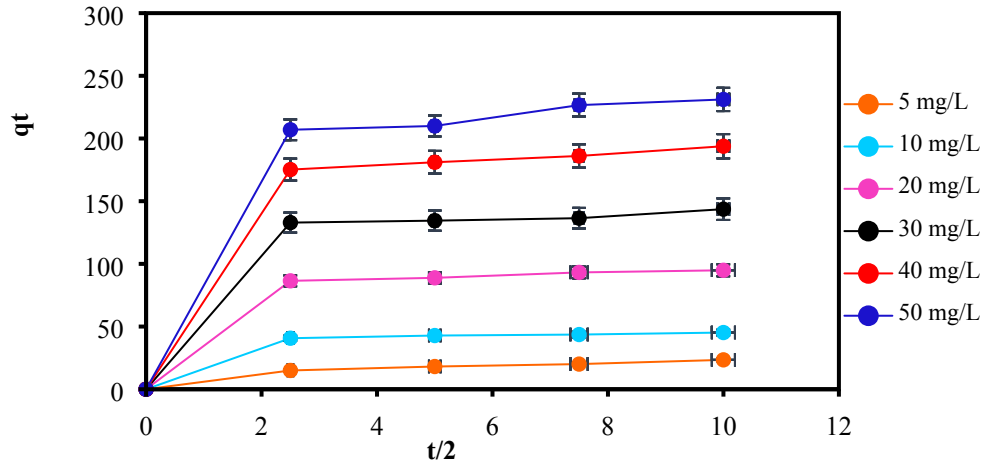


Fig. S3: Intraparticle diffusion model kinetics (a) dicamba and (b) MCPA (Dosage: 0.01 g/L; 40°C; equilibrium time: 25 min, rpm: 150)

Table S4: Kinetics parameters for the adsorption of dicamba and MCPA onto MIL-53(Al)

Kinetic Models		Dicamba					MCPA						
		5	10	20	30	40	50	5	10	20	30	40	50
<b>Pseudo-first-order</b>	$q_e$ exp (mg/g)	24.5	45.1	92.1	142.5	185.1	228.4	23.4	45.2	94.8	143.6	193.8	231.1
	$q_e$ cal (mg/g)	11.0	35.0	31.1	66.4	64.5	150.4	8.3	27.4	29.8	48.1	51.5	110.3
	$K_1$ (min) <sup>-1</sup>	0.1	0.1	0.1	0.1	0.1	0.1	0.1	0.1	0.1	0.1	0.1	0.1
	$R^2$	0.56	0.66	0.78	0.74	0.81	0.76	0.42	0.37	0.45	0.29	0.37	0.55
	$R^2$ adj	0.52	0.55	0.71	0.66	0.75	0.69	0.37	0.31	0.40	0.23	0.31	0.43
	RMSE	1.07	0.47	0.84	0.79	0.85	0.64	10.04	0.78	0.91	0.72	0.74	0.89
	AIC	3.5	-5.9	-0.2	-0.8	-0.1	-2.9	61.8	-4.6	-0.6	-6.5	-5.7	-1.1
<b>Pseudo-second-order</b>	$q_e$ cal (g mg/g)	25.1	42.9	91.7	142.8	185.1	227.2	20.7	45.2	95.2	142.8	192.3	232.5
	$K_2$ (g mg/ min <sup>-1</sup> )	0.1	0.0	0.0	0.0	0.0	0.1	0.1	0.1	0.0	0.0	0.1	0.1
	$R^2$	0.99	0.99	0.99	0.99	0.99	0.99	0.99	0.99	0.99	0.99	0.99	0.99
	$R^2$ adj	0.99	0.99	0.99	0.99	0.99	0.99	0.99	0.99	0.99	0.99	0.99	0.99
	RMSE	0.02	0.03	0.00	0.01	0.01	0.01	0.06	0.02	0.01	0.01	0.01	0.01
	AIC	-87.1	-87.1	-121.5	-109.5	-127.4	-133.8	-69.6	-90.1	-109.5	-121.1	-128.3	-131.5
<b>Intra-particle diffusion</b>	$K_p$ (mg/g min <sup>1/2</sup> )	1.5	2.6	5.4	8.4	10.9	13.6	2.1	3.7	7.8	11.6	15.9	19.2
	C	9.1	14.5	40.4	60.7	82.2	91.6	4.9	15.8	33.3	51.3	67.5	78.5
	$R^2$	0.33	0.48	0.26	0.29	0.25	0.33	0.47	0.28	0.27	0.27	0.28	0.29
	$R^2$ adj	0.26	0.43	0.19	0.22	0.19	0.27	0.42	0.21	0.21	0.21	0.22	0.22
	RMSE	5.81	9.33	22.64	34.30	45.828	53.24	5.05	10.99	23.18	34.94	46.94	55.79
	AIC	47.61	59.8	82.9	93.7	101.2	105.1	43.9	64.1	83.5	95.3	101.9	106.3



## Adsorption Isotherms

The equilibrium interaction between the analytes and the MIL-53(Al) MOF was studied based on the isotherm models. The values obtained are highlighted in Table S5. Based on the various results calculated, the Freundlich isotherm model (Fig. S4) best fit the adsorption process with the highest  $R^2 = 0.974\%$ ,  $0.962\%$ ;  $R^2_{adj} = 0.955$ ,  $0.953\%$ ; lowest RMSE  $< 0.079$ ,  $0.918$ ; and the least AIC  $< -28.875$ ,  $-18.279$  values for dicamba and MCPA, respectively. The Freundlich isotherms implies a multilayer interaction on a heterogeneous surface with different adsorption sites.

Table S5: Isotherm parameters for dicamba and MCPA adsorption onto MIL-53(Al)

Isotherm Model	Parameter	Dicamba	MCPA
Langmuir	$q_m$ (mg/g)	322.5	454.5
	$K_L$ (L mg/g)	0.4	0.3
	$R_L$	0.1	0.1
	$R^2$	0.23	0.40
	$R^2_{adj}$	0.04	0.20
	RMSE	0.01	0.01
	AIC	59.3	59.6
Freundlich	$K_F$ (mg/g)	5.9	7.7
	$n$	1.1	0.7
	$R^2$	0.97	0.96
	$R^2_{adj}$	0.95	0.95
	RMSE	0.07	0.19
	AIC	-28.8	-18.2
Temkin	$A$ (mg/g)	8.8	3.5
	$bT$ (kJ mol <sup>-1</sup> )	110.6	113.3
	$R^2$	0.71	0.74
	$R^2_{adj}$	0.63	0.68
	RMSE	48.16	46.48
	AIC	48.1	47.6

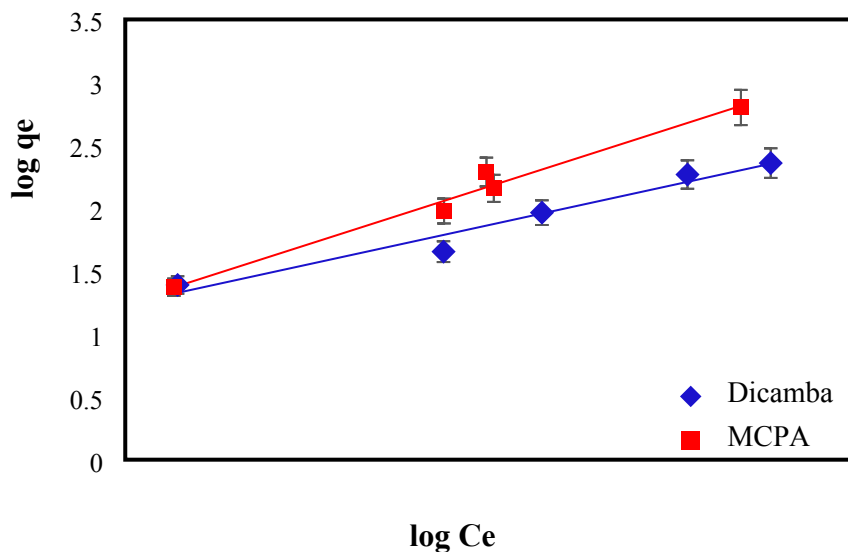


Fig. S4: Freundlich isotherms for the removal of (a) dicamba and (b) MCPA (Dosage: 0.01 g/L; 40°C; equilibrium time: 25 min; rpm: 150)

#### Thermodynamic studies

The thermodynamics values obtained are summarised in Table S6. The increase in temperature can impact on the pore capacity of the adsorbent as well as facilitate the number of cavity bubbles formed in the liquid bulk for easy dispersion. The  $\Delta G^\circ$  show negative values that indicate the spontaneous nature of the adoption process. The values obtained for  $\Delta H^\circ$  are positive ( $\Delta H^\circ = 55.57$  and  $49.12 \text{ KJ mol}^{-1}$ ) suggested that the adsorption of dicamba and MCPA on MIL-53(Al) follows an endothermic process. This depicts an increased randomness at the liquid-solid interface during the adsorption process.

Table S6: Thermodynamic parameters for the adsorption of dicamba and MCPA onto MIL-53(Al)

Temp (K)	Dicamba			MCPA		
	$\Delta G^\circ(\text{KJ mol}^{-1})$	$\Delta H^\circ(\text{KJ mol}^{-1})$	$\Delta S^\circ(\text{KJ mol}^{-1} \text{ K}^{-1})$	$\Delta G^\circ(\text{KJ/ mol}^{-1})$	$\Delta H^\circ(\text{KJ/ mol}^{-1})$	$\Delta S^\circ(\text{J/ mol}^{-1} \text{ K}^{-1})$
298	-51.5	55.5	172.6	-38.5	49.1	129.1
303	-52.3			-39.1		
308	-53.2			-39.8		
313	-54.1			-40.4		
318	-54.9			-41.1		
323	-55.8			-41.7		

#### References

- 1 Z. U. Zango, N. S. Sambudi, K. Jumbri, N. Hana, H. Abu, N. Ain, F. Abdullah, E. M. Negim and B. Saad, *Chem. Eng. Sci.*, 2020, **66**, 115608.
- 2 N. Delgado, A. Capparelli, A. Navarro and D. Marino, *J. Environ. Manage.*, 2019, **236**, 301–308.
- 3 Z. U. Zango, K. Jumbri, N. S. Sambudi, N. H. Hanif Abu Bakar, N. A. Fathihah Abdullah, C. Basheer and B. Saad, *RSC Adv.*, 2019, **9**, 41490–41501.